Modeling of the reverse gate leakage in AlGaN/GaN high electron mobility transistors

S. Sudharsanan and Shreepad Karmalkar

Citation: Journal of Applied Physics **107**, 064501 (2010); doi: 10.1063/1.3340826
View online: http://dx.doi.org/10.1063/1.3340826
View Table of Contents: http://scitation.aip.org/content/aip/journal/jap/107/6?ver=pdfcov
Published by the AIP Publishing

Modeling of the reverse gate leakage in AlGaN/GaN high electron mobility transistors

S. Sudharsanan[a] and Shreepad Karmalkar
Department of Electrical Engineering, Indian Institute of Technology, Madras 600 036, India

(Received 5 January 2010; accepted 28 January 2010; published online 16 March 2010)

The high gate leakage of AlGaN/GaN HEMTs grown on sapphire/SiC substrates having $x=0.2$, AlGaN thickness of 30 nm, and zero drain-source bias was earlier explained using the thermionic trap-assisted tunneling model. In the present work, we show that the same model can explain the gate leakage in AlGaN/GaN HEMTs grown on silicon substrates, having aluminum compositions of 24%, 26%, and 31%, AlGaN thickness of 20 nm, and drain-source bias (V_{DS}) of 10 V, over the gate-source voltages above threshold. © *2010 American Institute of Physics*. [doi:10.1063/1.3340826]

The bandgap of GaN is higher than that of GaAs, and so, the barrier height of the Schottky gate of $Al_xGa_{1-x}N/GaN$ HEMTs is higher than that of $Al_xGa_{1-x}As/GaAs$ HEMTs. However, the reverse gate leakage in $Al_xGa_{1-x}N/GaN$ devices is much higher than that in $Al_xGa_{1-x}As/GaAs$ devices.[1–3] Hence, modeling of this leakage in $Al_xGa_{1-x}N/GaN$ devices is important. The gate leakage is a function of the barrier height of the Schottky gate, the field beneath, and the quality of GaN and AlGaN layers. The Schottky barrier height is a function of the Al composition; the field beneath the gate depends on the device geometry and the applied gate and drain biases; the quality of GaN and AlGaN layers depend on the Al composition, substrate material (SiC, sapphire, or Si) and growth conditions.

Earlier, we have proposed a model of the gate voltage and temperature dependence of the reverse gate leakage of AlGaN/GaN HEMTs.[4,5] This model assumes thermionic trap-assisted tunneling (TTT) to be the leakage mechanism[4] and takes into account the two-dimensional (2D) field near the gate edge.[5] So far the model has been validated[4,5] on $Al_xGa_{1-x}N/GaN$ HEMT grown on a sapphire substrate having a specific aluminum composition ($x=0.2$) and AlGaN thickness (30 nm), and drain-source bias.[1] However, a good model of the gate leakage should explain the gate leakage behavior in a range of devices with different material compositions, device geometries, and bias conditions.

In the present work, we report the results of application of our gate leakage model for three AlGaN/GaN HEMTs grown on silicon substrates, having aluminum compositions of 24%, 26%, and 31%, AlGaN thickness of 20 nm, drain-source bias (V_{DS}) of 10 V, and moderate to high gate-source voltages (V_{GS}). All the three devices have the same dimensions as shown in Fig. 1 and their measured data were reported in Ref. 6. The following procedure is adopted for every device.

The AlGaN layer doping was adjusted to the values shown in Table I so that the threshold voltage extracted from linear extrapolation of the simulated I_{DS}-V_{GS} curve of the device for $V_{DS}=0.05$ V matched the measured threshold voltage. In this simulation, we assumed polarization charge equal to measured 2-DEG concentration, unintentional GaN doping of 1×10^{15} cm^{-3}, and conduction band discontinuity as per Anderson rule, and interpolated the electron affinity and bandgap for a given aluminum composition from those of GaN and AlN. Next, setting $V_{DS}=10$ V for each value of V_{GS}, the conduction band profile and electric field along the vertical (gate to substrate) direction are simulated using ATLAS 2D at several points over the gate length. The number of points chosen is considered sufficient, if any increase in this number does not cause a change in the current calculated in the final step. More points are chosen near the edges than in the middle of the gate to accurately capture the rapid variations in the field, and hence the current density, at the gate edges. The shape of the potential barrier formed by the simulated conduction band profile (at any of these points) is nontriangular in shape (see Fig. 2).

Some values of trap concentration N_t and trap energy ϕ_t are assumed as initial guess. The tunneling current densities through the simulated potential barriers at various points along the gate length are calculated using MATLAB based on the following TTT equation[4] applicable for an arbitrary shaped barrier,

$$J_{TTT} = qC_tN_t\int_{x_t}^{\infty}\left(\frac{1}{f_{FD}(x_2)P_1(x_2)}+\frac{1}{P_2(x_2)}\right)^{-1}dx_2. \qquad (1)$$

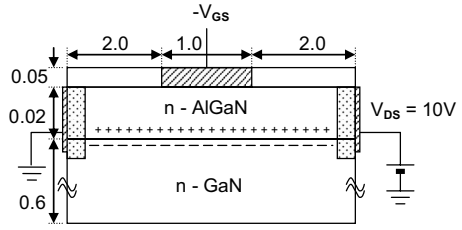

FIG. 1. AlGaN/GaN HEMT structure with nonzero V_{DS} used in Ref. 6 for gate leakage measurements and in this work for simulation. Device dimensions are in microns. Doping in the source/drain region is assumed to be 1×10^{19} cm^{-3}. Figure is not to scale.

[a]Electronic mail: sudharsanan87@gmail.com. Tel.: 91-44-2257-4409. FAX: 91-44-2257-4402.

TABLE I. Measured and extracted parameter values in the present and an earlier work (Ref. 3). The devices of the present work were grown on Si substrates, had AlGaN thickness of 20 nm, and V_{DS}=10 V; the corresponding parameters of the device in the earlier work are SiC substrate, 30 nm, and 0 V.

	Measured parameters		Extracted/calculated parameters				
Al composition	V_T (V)	2-DEG density (cm^{-2})	AlGaN doping (cm^{-3})	Trap energy ϕ_t (V)	Trap density N_t (cm^{-2})	Barrier Height ϕ_B (V)	Reference
0.24	−0.40	3×10^{12}	1.8×10^{17}	0.90	8.0×10^{17}	1.60	Present work
0.26	−1.29	4.6×10^{12}	7.0×10^{17}	0.91	9.0×10^{17}	1.64	
0.31	−2.14	7.4×10^{12}	2.0×10^{16}	1.10	6.0×10^{18}	1.75	
0.20	−2.50	2.59×10^{12}	2.0×10^{18}	0.845	1.38×10^{16}	1.52	5

This equation is the result of introducing the Fermi–Dirac function f_{FD} into the trap-assisted tunneling equation to incorporate the thermally activated electrons; C_t is the trap energy dependent rate constant, P_1 and P_2 are the tunneling probabilities based on WKB approximation for a two-step tunneling process through the barrier, and locations x_t, x_1, and x_2 are defined in Fig. 3. The terms f_{FD}, P_1, P_2, and C_t are given by

$$f_{FD}(x_2) = \frac{1}{1+\exp\{q[\phi_B - \phi(x_2)]/kT\}}, \tag{2}$$

$$P_1(x_2) = \exp\left\{-\alpha\int_0^{x_1}\sqrt{[\phi(x_2)-\phi(x)]}dx\right\}, \tag{3}$$

$$P_2(x_2) = \exp\left\{-\alpha\int_{x_1}^{x_2}\sqrt{[\phi(x_2)-\phi(x)]}dx\right\}, \tag{4}$$

$$\alpha = \frac{4\pi\sqrt{2mq}}{h}, \quad C_t = \left(\frac{m_M}{m_S}\right)^{5/2}\frac{16\pi q\phi_1^{3/2}}{3h\sqrt{\phi_t-\phi_1}}, \tag{5}$$

$$\phi_1 = 0.2 \text{ V}.$$

Here m_S and m_M denote the effective mass of electron in semiconductor and metal respectively; effective electron mass is assumed to be a constant throughout the tunneling process. Due to the presence of f_{FD}, Eq. (1) defies analytical integration and so is evaluated numerically. Finally, the gate current is calculated by numerically integrating the current density over the gate length. The tunneling along lines at an angle to the gate edge is neglected[5] because the electrons have to go through the dielectric layer (Si_3N_4 in our case) present near the gate edge, and thus encounter a high barrier. The trap parameters N_t and ϕ_t are adjusted to the values shown in Table I to fit the calculated current to the measured data.

Figure 4 shows that the fit between the calculated and measured data is good over most of the V_{GS} range, except at low V_{GS} (below threshold) the reasons for which are unclear at this time and need to be investigated. Table I shows that the extracted values of N_t and ϕ_t are realistic, but the values of N_t in the present work are larger than those in our earlier work.[3] The latter is due to the different substrates used in the two works. The devices in the present work were made on silicon substrates, which introduce a larger lattice mismatch in the layers grown over the substrate than sapphire substrates employed in the earlier work.[1,4,5] Another notable observation is that the measured gate current increases with an increase in aluminum composition, i.e., with increasing barrier height. This rules out direct tunneling, i.e., thermionic

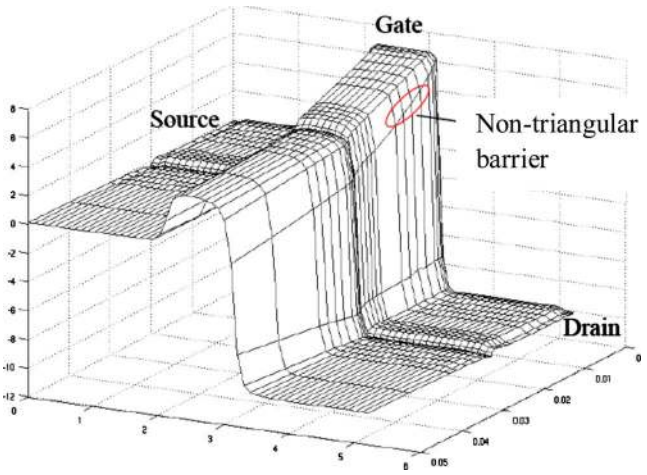

FIG. 2. (Color online) Simulated conduction band profile within the device depicting the nontriangular shape of the gate potential barrier.

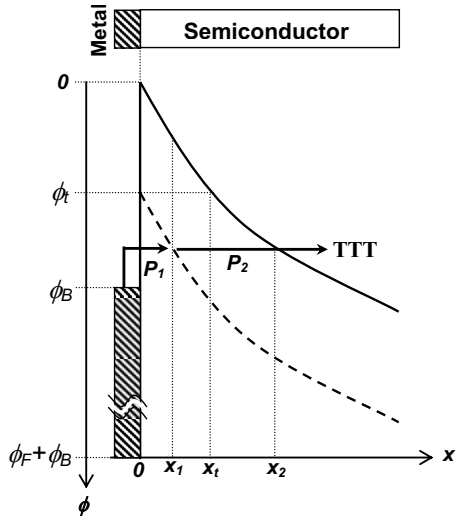

FIG. 3. Energy band diagram of a reverse biased metal semiconductor junction depicting TTT; ϕ_t is the trap ionization energy, ϕ_B is the barrier height, and $\phi=\phi_F+\phi_B$ is the bottom of the conduction band in metal. Locations x_1, x_2, and x_t are used as integration limits in TTT and DT model equations.

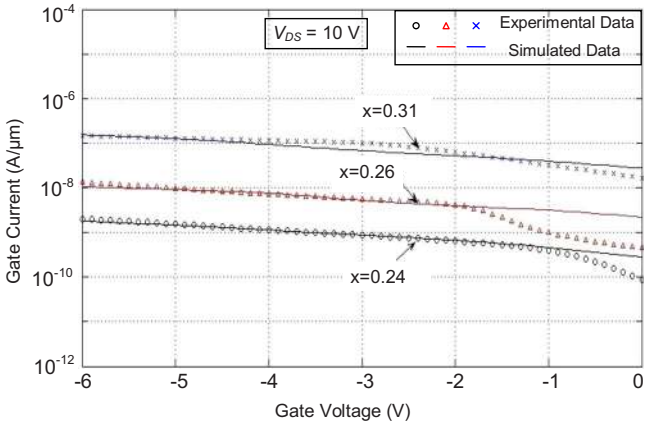

FIG. 4. (Color online) Simulated (lines) and measured (points) currents for the three devices reported in Ref. 6.

field emission (TFE), as a possible mechanism of gate current transport since TFE decreases with increase in barrier height. Also, the TFE current calculated taking into account the edge field turns out to be much higher than the TTT current. Thus, TTT is indeed the more appropriate mechanism for gate leakage.

In conclusion, the present work has extended the validity of the TTT model proposed earlier by us for the gate leakage in AlGaN/GaN HEMTs, by considering devices with different substrates, aluminum compositions, and drain-source bias.

One of the authors, Sudharsanan S., would like to thank Dr. D. M. Sathaiya for helpful discussions.

[1]S. Mizuno, Y. Ohno, S. Kishimoto, K. Maezawa, and T. Mizutani, Jpn. J. Appl. Phys., Part 1 **41**, 5125 (2002).
[2]E. J. Miller, X. Z. Dang, and E. T. Yu, J. Appl. Phys. **88**, 5951 (2000).
[3]M. S. Shur, A. D. Bykhovski, R. Gaska, and A. Khan, in *Handbook of Thin Film Devices*, edited by C. E. C. Wood and M. H. Francombe (Academic, San Diego, 2000), Vol. 1, p. 299.
[4]D. Mahaveer Sathaiya and S. Karmalkar, J. Appl. Phys. **99**, 093701 (2006).
[5]D. M. Sathaiya and S. Karmalkar, IEEE Trans. Electron Devices **54**, 2614 (2007).
[6]M. Fieger, M. Eickelkamp, L. Rahimzadeh Koshroo, Y. Dikme, A. Noculak, H. Kalisch, M. Heuken, R. H. Jansen, and A. Vescan, J. Cryst. Growth **298**, 843 (2007).